Solar Phys (2007) 241: 251–261
DOI 10.1007/s11207-007-0250-6

Filamentary Structures of Coronal White-Light Images

Richard Woo

Received: 27 June 2006 / Accepted: 15 April 2007 /
Published online: 29 May 2007

Abstract In the absence of magnetic field measurements of the solar corona, the density structure of white-light images has provided important insight into the coronal magnetic field. Recent work sparked by highly sensitive radio occultation measurements of path-integrated density has elucidated the density structure of unprocessed solar eclipse pictures. This paper does the same for processed images that reveal low-contrast small-scale structures, specifically Koutchmy's edge-enhanced white-light image of the 11 August 1999 solar eclipse. This processed image provides visual evidence for two important results deduced from radio occultation measurements of small-scale density variations. First, in addition to the closed loops readily seen at the base of the corona in high-resolution EUV and soft X-ray images, open filamentary structures permeate the corona including active regions generally thought to be magnetically closed. Observed at the image resolution, the filamentary structures are 1° wide in latitude and an order of magnitude smaller than polar plumes. Second, although inhomogeneities that are convected along with the solar wind are also present, filamentary structures dominate the image because of their steeper density gradients. The quantitative profile of polarized brightness (pB) at the base of the corona shows that the filamentary structures have transverse density gradients that are proportional to their density. This explains why edge-enhanced images, limited in sensitivity to density gradients, tend to detect filamentary structures more readily in high-density regions (*e.g.*, active regions, streamer stalks, and prominences) than in low-density polar coronal holes, and why filamentary structures seem more prevalent in solar eclipse pictures during solar maximum. The pB profile at the base of the corona also fills the gap in Doppler measurements there, reinforcing that open ultra-fine-scale filamentary structures observed by the radio measurements are predominantly radial and that they are an integral part of the radial expansion of the solar wind.

R. Woo (✉)
Jet Propulsion Laboratory, California Institute of Technology, 4800 Oak Grove Drive, MS 238-725, Pasadena, CA 91109, USA
e-mail: richard.woo@jpl.nasa.gov

1. Introduction

Recent progress has demonstrated how relating complementary white-light and radio occultation measurements of path-integrated electron density mutually benefits understanding coronal plasma density. (Note that we use density and path-integrated density interchangeably in this paper.) In particular, it has demonstrated the importance of quantitative profiles in elucidating the density structure of solar eclipse pictures, as stressed by early investigators (*e.g.*, Mentzel, 1959; Newkirk, Dupree, and Schmahl, 1970). Specifically, it has shown how the size and the shape of the imaged white-light corona reflects the sensitivity or signal-to-noise ratio limitation of the observing instrument, in addition to the influence of the coronal magnetic field and plasma flow (Woo, 2005).

When white-light images are processed, *e.g.*, by edge enhancement, they reveal a corona that is filled with striking and puzzling small-scale features. These include filamentary structures (Koutchmy *et al.*, 1992, 1993; Guhathakurta and Fisher, 1995; November and Koutchmy, 1996; Morgan, Habbal, and Woo, 2006) and inhomogeneities or blobs that are convected along with the solar wind (Sheeley *et al.*, 1997). Why does the corona in processed images look so different from that of unprocessed images?

The purpose of this paper is to address this issue and the following additional questions. Why are small-scale structures revealed more readily only when white-light images are processed, and how are they related to those observed by radio occultation measurements? Is there visual evidence for the open structures inferred from radio occultation measurements (Woo, 2006), and along which the solar wind expands radially from the Sun? Are the imaged small-scale structures affected by instrumental limitations, and, if so, in what way and with what implications? How are quantitative profiles of density related to the small-scale structures, and what can we learn from them?

2. White-Light Measurements

This investigation of small-scale structure is based on white-light measurements of the 11 August 1999 solar eclipse (Habbal *et al.*, 2001; Koutchmy *et al.*, 2001). As with unprocessed images (Woo, 2005), we use both imaging and quantitative profiles to elucidate the structure of processed images, and we discuss them separately.

2.1. Edge-Enhanced Image

Shown in Figure 1a is a composite of the ground-based and SOHO LASCO C2 images of path-integrated density for the 11 August 1999 solar eclipse. Koutchmy *et al.* (2001) obtained Figure 1b by using an algorithm that enhances the contrast (Koutchmy and Koutchmy, 1989), a process also known as edge enhancement. Since the eclipse took place during solar maximum when streamers appeared at all latitudes, the coronal structure appears especially rich. As discussed by Woo (2005), the boundaries of the coronal shape outlining the seemingly tapering streamers do not trace the magnetic field but are artifacts of the sensitivity-limited camera; these are accentuated when the image is edge enhanced. In contrast, the small-scale filamentary structures that are bounded by steep transverse density gradients are presumably tracers of the magnetic field.

The filamentary structures that permeate the corona at the image resolution of Figure 1b are approximately 1° in latitude (12 Mm or 17″ at the Sun). They are an order of magnitude smaller than the 10° wide polar plumes associated with polar coronal holes (Fisher and

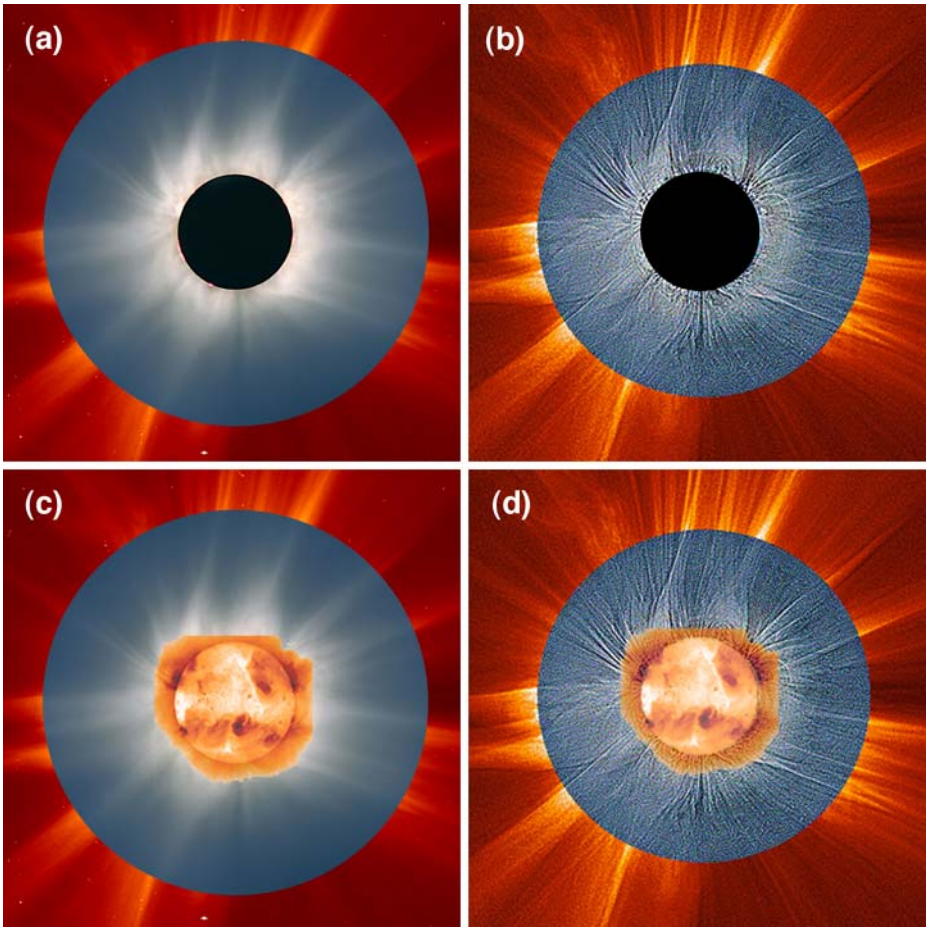

Figure 1 (a) Combined eclipse and SOHO LASCO C2 white-light images of the 11 August 1999 total solar eclipse, with north pointing up (courtesy of S. Koutchmy). Occurring during solar maximum, the corona shows streamers at all latitudes. (b) Edge-enhanced image (courtesy of S. Koutchmy) revealing filamentary structures at the image resolution that are 1° wide in latitude. In addition to the low-lying closed loops, striking open filamentary appear to emanate from the entire Sun. The *Yohkoh* image of the solar disk is superposed on the images of (a) and (b) and shown in (c) and (d), respectively. The open filamentary structures associated with the active regions on the northeast and northwest limb are especially pronounced and surprising, since active regions are widely thought to be magnetically closed.

Guhathakurta, 1995; Woo, 1996a; DeForest, Lamy, and Llebaria, 2001). Like earlier eclipse pictures during solar maximum (*e.g.*, Figure 14 of Koutchmy *et al.*, 1992), the most striking feature of Figure 1b is that, in addition to low-lying closed loops, the corona is pervaded by predominantly radial filamentary structures tracing open magnetic field lines. These open filamentary structures are apparently characterized by a low filling factor, and we will discuss this in conjunction with the radio occultation measurements in Section 3.2.

This impression of white-light images stands in stark contrast with that of high-resolution EUV and soft X-ray images in which closed loops dominate (see, *e.g.*, Aschwanden, 2004). This is not surprising in view of the fact that the measurements are of fundamentally different processes. White-light images depict white light scattered by the coronal plasma. Because

closed and open filamentary structures are both bounded and characterized by steep transverse density gradients, the scattered white light of edge-enhanced white-light images does not favor one or the other. It shows, therefore, a truer picture of the filamentary structures that trace the coronal magnetic field: a mixture of low-lying closed fields and open fields that appear to emanate from the entire Sun.

Unlike white light, which observes total density, emission reflects both density and temperature. We still do not fully understand why and how some filamentary structures are lit up in emission images whereas others are not, or why multitemperature structures are not co-spatial (Habbal, 1994). Several reasons may explain the dominance of emission images by closed structures. Since emission is proportional to the square of density and white light is proportional to density, the fainter emission from open structures especially farther from the Sun may be harder to detect. Closed structures may also appear more readily in emission images because of fundamental differences between the open and closed structures. Open structures are likely to be cooler on account of efficient plasma transport, whereas closed structures are hotter because heated plasma is trapped and cannot easily flow away.

The corresponding *Yohkoh* soft X-ray image showing the active regions at the limb of the Sun is superposed on Figures 1a and 1b and displayed in Figures 1c and 1d, respectively. Although active regions are generally thought of as exclusively closed (*e.g.*, Uchida *et al.*, 1992), open filamentary structures extending from them and their vicinity are seen in Figure 1d. Because of projection effects, we cannot rule out the possibility that the filamentary structures associated with active regions may instead be associated with other places hidden behind the limb. However, in contrast to solar eclipse pictures, which provide information only on latitudinal variation, radio occultation measurements observe the corona as the Sun rotates, and the observed longitudinal variation is consistent with open filamentary structures being confined to the vicinity of active regions (Woo, 2006).

Open filamentary structures are associated with the active region on the northwest limb that underlies a streamer, as well as the active region on the northeast limb that does not. As discussed by Woo and Habbal (2005), the former corresponds to the case where the heliospheric current sheet is transverse to the plane of the sky, and the latter to the case where the sheet is in the plane of the sky. That the presence of open filamentary structures is independent of the orientation of the heliospheric current suggests that the filamentary structures associated with the active regions are individual raylike structures rather than sheets observed edge-on. They presumably trace the open field lines implied by the appearance of the imprint of active regions in the solar wind (Woo, Habbal, and Feldman, 2004), and along which the slow wind flows (Woo and Habbal, 2005).

2.2. Quantitative Profiles

Although Figure 1b offers visual evidence for the filamentary structures, quantitative profiles of polarized brightness *pB* provide the opportunity to characterize them near the base of the corona where the signal-to-noise ratio is strongest. Shown in Figure 2a is the latitudinal profile of *pB* at 1.15 $R_{\odot}$ reported by Habbal *et al.* (2001), plotted as a function of position angle (PA) in 1° increments measured counterclockwise from 0° North. Superposed on the profile of Figure 1a are relatively small fluctuations, which at first glance seem to represent measurement uncertainty or noise. However, the peak-to-peak variations in their derivative shown in the upper curve of Figure 1a are not uniform as they would be for noise. Instead, the derivative of *pB*, which measures the transverse or latitudinal density gradients that bound the $\approx 1°$ scale filamentary structures, shows significant variation with position angle. Filamentary structures are hidden in Figure 1a, not because they are faint, but because their

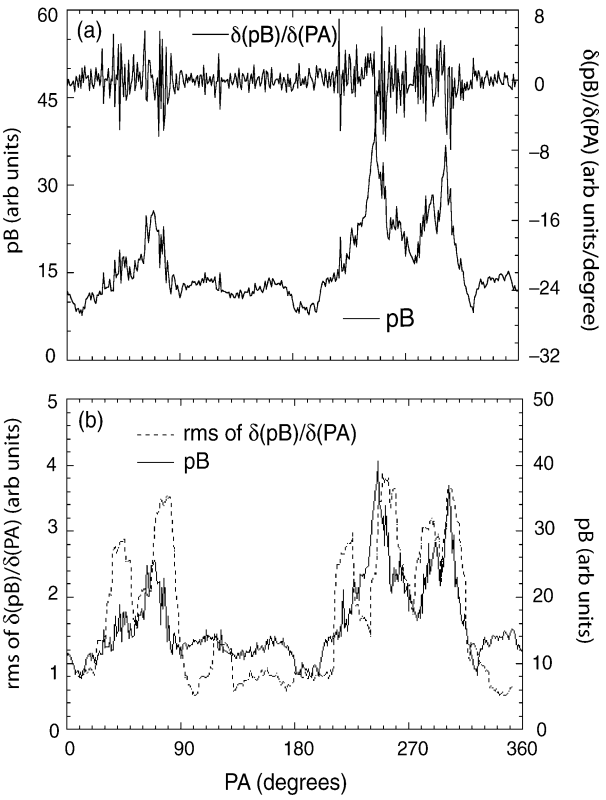

Figure 2 (a) The lower curve shows polarized brightness *pB* near the base of the corona at 1.15 R_o as a function of position angle PA, measured counterclockwise from 0° North in increments of 1°. It represents the variation in large-scale density portrayed in Figure 1a. Variation of the derivative of *pB* with respect to PA is shown in the upper curve. It represents the variation in transverse density gradients bounding the small-scale structures revealed in Figure 1b. (b) The rms of *pB* in (a) computed in a sliding window 15° wide and superposed on the curve of *pB*. The striking correlation between the two curves indicates that filamentary structures at the base of the corona have transverse density gradients reflecting their density and hence the complexity and strength of the magnetic field.

density levels differ little from those of their neighboring structures. Since they are characterized by steep transverse density gradients rather than density, filamentary structures are more readily revealed in the edge-enhanced image of Figure 1b.

Shown in Figure 2b is the sliding rms of the variations in the derivative of *pB* computed over a latitudinal range of 15°, along with the latitudinal profile of *pB*. The latitudinal range for computing the rms is not critical; it has been chosen high enough to reduce uncertainty in the rms calculation, and sufficiently low for reasonable spatial resolution. The two results in Figure 2b are clearly correlated, and a scatter plot analysis shows that the correlation coefficient exceeds 0.8. This high correlation indicates that the filamentary structures at the base of the corona have transverse density gradients that are proportional to their density. It applies to both open structures and the legs of closed structures, since the two are indistinguishable in the *pB* profile. The three regions of highest density and steepest gradients correspond to active regions located near PA 70°, 245°, and 300°, explaining why the filamentary structures associated with active regions seem particularly distinct in the images of Figures 1b and 1d.

That transverse density gradients are steepest in regions of highest density explains why low-contrast filamentary structures are seen more readily in processed white-light images of streamers (Koutchmy *et al.*, 1992; Guhathakurta and Fisher, 1995), prominences (November and Koutchmy, 1996), and coronal mass ejections (Morgan, Habbal, and Woo, 2006), in addition to active regions. Higher density (Hansen *et al.*, 1969) is also the reason why filamentary structures seem more prevalent during solar maximum, as evident in Figure 1b. The

ubiquitous filamentary structures are consistent with the fibrous corona invoked to explain the observations of solar radio emission, and their steepest transverse gradients explain why beaming or guided wave propagation is most likely to occur in active regions (*e.g.*, Bougeret and Steinberg, 1977; Roelof and Pick, 1989; Wu *et al.*, 2004).

3. Relating White-Light and Radio Measurements

Figure 2a is reproduced in Figure 3 along with ranging and Doppler measurements from Woo (2006). Ranging measures path-integrated density and Doppler observes changes in path-integrated density at a point that moves across the plane of the sky. As in the case of the large derivative of *pB* variations, the large Doppler fluctuations, reflecting large density gradients observed in the outer corona near 30 R_o as the Sun rotates, overlie an active region (Woo, 2006). The similarities between the white-light and radio measurements are striking, especially because the white-light results represent strictly spatial variation while the radio results represent temporal variation. They illustrate the spatial-temporal ambiguity of radio occultation measurements that has hindered progress in relating radio and white-light measurements for a long time (Woo, 1996b; Woo, Armstrong, and Gazis, 1995). In the following we discuss how the results of this paper further elucidate the close relationship between these two powerful measurements, and how they mutually benefit the understanding of both techniques.

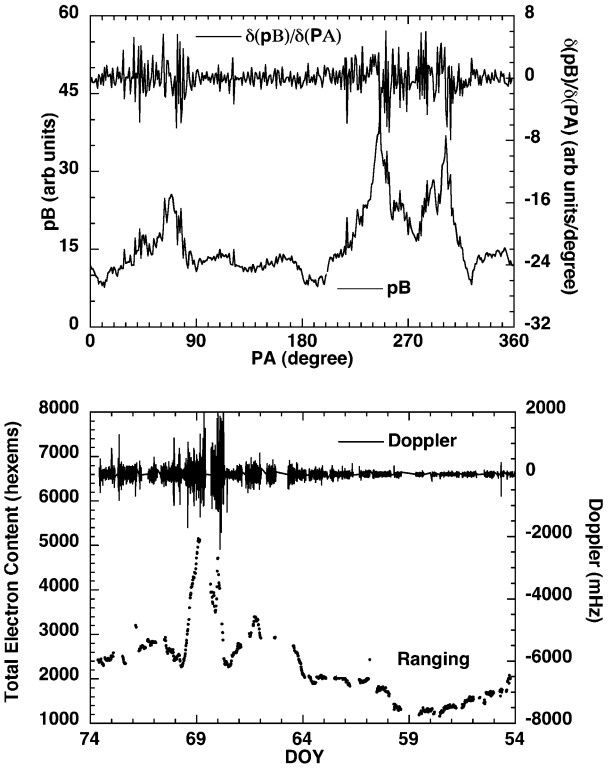

Figure 3 Upper panel is the reproduction of Figure 2a. Lower panel shows ranging measurements of path-integrated density and Doppler measurements of changes in path-integrated density as a function of day of year DOY in 1995 adapted from Figure 1 of Woo (2006). Like the regions of large variations in the derivative of *pB*, the region of large variation in Doppler fluctuation overlies an active region. The striking similarity between the radio and white-light results demonstrates the close association between the two; it also illustrates how spatial-temporal ambiguity can confuse radio measurements, since the *pB* variations are latitudinal or spatial, whereas the radio variations observed at a point in the plane of the sky are temporal.

3.1. How White Light Complements Radio

Figure 1b provides visual evidence for two of the most important results from radio occultation measurements. It reveals that open filamentary structures pervade the solar corona in addition to low-lying closed loops. These structures are detected in Doppler measurements such as those shown in Figure 3, because their steep transverse density gradients impose corresponding large Doppler shifts in the radio signal when they rotate across the radio path. The time scale is set by the solar rotation, and the 1° wide structures of Figure 1b translate into a time scale of 2 hours or a fluctuating frequency of 1.6×10^{-4} Hz. The white-light filamentary structures, therefore, represent the large-scale end of the size distribution of filamentary structures detected in Doppler measurements, the finest being around 4 orders of magnitude smaller (Woo, 1996b; Woo and Habbal, 1997a).

As revealed in time-lapse white-light images (Sheeley *et al.*, 1997), the corona comprises inhomogeneities or blobs convected along with the solar wind in addition to filamentary structures. Edge-enhanced Figure 1b, therefore, provides visual evidence for the second important conclusion from radio occultation measurements. Although they coexist, filamentary structures, rather than propagating inhomogeneities or turbulence, dominate small-scale coronal density structure because of their steeper density gradients (Woo, 1996b). If turbulence dominated, the corona in Figure 1b would appear more randomized instead of highly structured and filamentary.

The quantitative profile of pB in Figure 2b also complements radio occultation measurements in two significant ways. Doppler measurements showed (Woo, 2006) that the open filamentary structures observed by them in the outer corona had transverse density gradients proportional not only to their own density, but also to the density at the base of the corona underlying them. This suggested that the filamentary structures extended from the underlying corona and were hence predominantly radial. What was missing to confirm this was evidence to show that the transverse density gradients of the filamentary structures at the base of the corona were also proportional to their density, and the profile of pB in Figure 2b provides it.

Global radio occultation measurements of angular broadening (Erickson, 1964; Newkirk, 1967), intensity scintillation (Bourgois, 1969; Hewish, 1972), Doppler scintillation (Woo, 1978) and other radio scattering phenomena have long suggested that small-scale coronal density variations are proportional to density. The second significant way in which the quantitative profile of pB at 1.15 R_o complements the radio occultation measurements is that it shows that the source of this proportionality is the Sun.

3.2. How Radio Complements White Light

If we look at their sensitivity, it is easy to understand why radio occultation measurements are so powerful for investigating small-scale structure. As mentioned earlier the 1° structures, which are barely detected in white-light images, correspond to a fluctuating frequency of 1.6×10^{-4} Hz in the Doppler or phase (integrated Doppler) measurements. The signal-to-noise ratio (*i.e.*, power in the phase fluctuations near 10^{-4} Hz divided by the power in the thermal noise of the radio receiver) is at least 10^{10} (see Figure 3 of Woo and Armstrong, 1979). The density variations or density gradients are significantly smaller for the finer scales, but even in the case of the smallest 1-km filamentary structures that correspond to a fluctuating frequency of about 1 Hz, the signal-to-noise ratio exceeds 100 (see Figure 3 of Woo and Armstrong, 1979). This extraordinary signal-to-noise ratio of Doppler

measurements accounts for why they provide a more complete picture of coronal small-scale structure. Permeating the entire corona throughout the solar cycle, open filamentary structures are the building blocks of the solar wind.

Image resolution clearly limits the investigation of small-scale structures with white-light measurements. What is less obvious is the fact that filamentary structures can go undetected, not because they are too small, but because the observing instrument is limited in sensitivity to density gradients. These missing structures can give false impressions of the solar corona. For instance, based on solar eclipse pictures, we do not know that filamentary structures pervade polar coronal holes in addition to polar plumes, as is evident in simultaneous ranging and Doppler measurements (Woo and Habbal, 1997b). Solar eclipse images also falsely portray a corona that seems more filamentary during high solar activity, when Doppler measurements show that filamentary structures are present everywhere and at all times.

Coexisting small-scale inhomogeneities that are convected with the solar wind are observed by multiple-station intensity scintillation measurements (Dennison and Hewish, 1967; Grall *et al.*, 1996). Like filamentary structures, these moving inhomogeneities are observed by high-sensitivity radio measurements everywhere in the corona and throughout the solar cycle. Time-lapse sequences of white-light images of larger inhomogeneities during solar minimum have been used to extract estimates of solar wind speed in a similar manner (Sheeley *et al.*, 1997), but because of limitations in detecting density gradients, these have been restricted mainly to coronal streamer stalks where density gradients are large. If time-lapse white-light measurements were our only means for observing plasma flow, we might have erroneously concluded that the solar wind flowed only from streamer stalks.

The appearance of polar plumes in polar coronal holes of white-light images (Van de Hulst, 1950; Saito, 1965; Newkirk and Harvey, 1968, DeForest, Lamy, and Llebaria, 2001) is generally thought to imply that polar coronal holes are the only source of open field lines, with the corona being closed everywhere else (Hundhausen, 1977; Munro and Jackson, 1977). The filamentary structures detected by Doppler measurements, but missing from these images on account of inadequate sensitivity to density gradients, have important implications for the solar wind. While the larger polar plumes seem to be confined to polar coronal holes and related to the network (Newkirk and Harvey, 1968), the filamentary structures pervade the entire corona. If the filamentary structures are the building blocks that fill the entire corona, why do those in the edge-enhanced white-light image of Figure 1b have a low filling factor?

As with the closed loops of high-resolution emission images, the low filling factor of filamentary structures of edge-enhanced white-light images appears to be associated with the spatial intermittency of the photospheric field (Golub and Pasachoff, 1997). This connection is suggested by the similarity between the density spectra of filamentary structures inferred from Doppler measurements (Woo, 2006) and the spatial spectra of the photospheric field (Abramenko *et al.*, 2001). Spatial intermittency of the photospheric field seems to be characterized in the solar corona more by enhancements in emission and transverse density gradients than by enhancements in density of the filamentary structures.

In contrast to polar plumes, the extensions of the ubiquitous filamentary structures into interplanetary space that form the shape of the corona of sensitivity-limited white-light images (Woo, 2005), and the transverse density gradients of the filamentary structures that lead to their detection in edge-enhanced white-light images, reflect the magnetic field complexity at the base of the corona. Thus, in active regions where magnetic plasma trapping is most prolonged, the filamentary structures are longer, brighter, and more distinct. These differences between the properties of filamentary structures and the larger polar plumes reinforce that the former must have a more fundamental role in the origin and evolution of the solar wind.

4. Conclusions

Coronal imaging has strongly influenced our notions of magnetic fields and plasma flow in the solar corona. For a long time, streamers and plumes of solar eclipse images seemed to suggest, and recent high-resolution emission images of low-lying closed loops seemed to reinforce, that the coronal magnetic field was not only open and highly non-radial in polar coronal holes, but exclusively closed everywhere else. This picture began to undergo change with the elucidation of density structure by highly sensitive and high time resolution ranging and Doppler measurements of density and density changes, respectively. Instead, the solar wind was found to expand radially from the entire Sun along predominantly radial filamentary structures detected by Doppler measurements (Woo, 2006). Radial expansion from the Sun was manifested in the radial extension into interplanetary space of the signatures of coronal holes, quiet Sun, and active regions representing the imprint of the Sun (Woo and Habbal, 2001; Woo, Habbal, and Feldman, 2004), and reinforced by the predominantly radial direction of the coronal magnetic field inferred from polarization measurements (Eddy, Lee, and Emerson, 1973; Habbal, Woo, and Arnaud, 2001). The false impressions of highly non-radial magnetic fields shaping the corona in eclipse images have since been reconciled with radial expansion by realizing that the shape of the corona is the combined consequence of the sensitivity limitation of the observing instrument and the large variation in radial density gradient with latitude (Woo, 2005).

Although processed white-light images have always shown a corona that is highly structured with small-scale features, the implications of these small-scale structures for magnetic fields and plasma flow were seldom considered or discussed. One reason for this lack of discussion might have been that they and the artifacts of image processing were not well understood, but another reason may have been that open structures were at odds with the notion that coronal regions other than coronal holes were magnetically closed. In this paper, we have further demonstrated the mutual benefits of relating radio and white-light measurements by taking a closer look at the low-contrast small-scale structures using the edge-enhanced image of 11 August 1999 and integrating them into the new context of coronal density structure inferred from Doppler measurements.

The 1° wide filamentary structures of this edge-enhanced image are an order of magnitude smaller than polar plumes, but they correspond to the large-scale end of the size distribution of those detected by Doppler measurements. Still, they provide visual evidence not only for the presence of open filamentary structures in the corona including active regions thought to be magnetically closed, but also for their dominance over coexisting moving inhomogeneities because of steeper density gradients. The visual evidence for open filamentary structures is especially important in light of its absence from emission images. The agreement between the larger scales observed by white-light and the smaller scales observed by Doppler measurements suggests that, like the closed loops of emission images, the open filamentary structures are self-similar. This is also consistent with the single power-law characterization of the filamentary structures (Woo, 2005). The similarity between the latter and the spatial spectra of the photospheric field provides an explanation for why the low filling factor of the filamentary structures in edge-enhanced white-light images appears to be a manifestation of the spatial intermittency of the photospheric field.

Because of their extraordinary sensitivity and time resolution, Doppler measurements show a more complete picture of the corona, one in which filamentary structures permeate the entire corona throughout the solar cycle. The sensitivity limitation to density gradients and the fact that density gradients are proportional to density, combine to explain why filamentary structures tend to appear more readily in high-density regions such as streamers, prominences, and active regions than in polar coronal holes.

In conclusion, the radial extension of the imprint of the Sun is the most robust observational evidence for the radial expansion of the solar wind. Rather than relying on images of selected individual small-scale structures, it represents the collective consequence of all of them, regardless of whether they are detected or not. Nevertheless, when compared with unprocessed images of the corona, like Doppler to ranging measurements, edge-enhanced images of filamentary structures offer independent and more direct observations of the coronal magnetic field. Although limited by spatial resolution and sensitivity, the visual evidence of the open filamentary structures reassures us that the corona-wide ultra-fine-scale filamentary structures detected by Doppler measurements trace the open magnetic field lines along which the imprint of the Sun is carried radially into interplanetary space.

Acknowledgements This research was carried out at the Jet Propulsion Laboratory (JPL), California Institute of Technology, under contract with the National Aeronautics and Space Administration and funded through the Internal Research and Technology Development Program. It is a pleasure to thank C. Copeland for producing the figures, S.R. Habbal for the *pB* profiles, S. Koutchmy for the coronal images, the *Yohkoh* Data Archive Center for the *Yohkoh* soft X-ray images, and J.W. Armstrong and S.R. Habbal for many useful discussions. The SOHO/LASCO data used here are produced by a consortium of the Naval Research Laboratory (USA), Max-Planck-Institut für Aeronomie (Germany), Laboratoire d'Astronomie (France), and the University of Birmingham (UK). SOHO is a project of international cooperation between ESA and NASA. I would also like to acknowledge the JPL sabbatical program, without which the work reported here would not have been possible.

References

Abramenko, V., Yurchyshyn, V., Wang, H., Goode, P.R.: 2001, *Solar Phys.* **201**, 225.
Aschwanden, M.J.: 2004, *Physics of the Solar Corona*, Praxis, Chichester.
Bougeret, J.L., Steinberg, J.L.: 1977, *Astron. Astrophys.* **61**, 777.
Bourgois, G.: 1969, *Astron. Astrophys.* **2**, 209.
DeForest, C.E., Lamy, P.L., Llebaria, A.: 2001, *Astrophys. J.* **560**, 490.
Dennison, P.A., Hewish, A.: 1967, *Nature* **213**, 343.
Eddy, J.A., Lee, R.H., Emerson, J.D.: 1973, *Solar Phys.* **30**, 351.
Erickson, W.C.: 1964, *Astrophys. J.* **139**, 1290.
Fisher, R.R., Guhathakurta, M.: 1995, *Astrophys. J.* **447**, L139.
Golub, L., Pasachoff, J.: 1997, *The Solar Corona*, Cambridge University Press, Cambridge, 202.
Grall, R., *et al.*: 1996, *Nature* **379**, 429.
Guhathakurta, M., Fisher, R.R.: 1995, *Geophys. Res. Lett.* **22**, 1841.
Habbal, S.R.: 1994, *Space Sci. Rev.* **70**, 37.
Habbal, S.R., Woo, R., Arnaud, J.: 2001, *Astrophys. J.* **558**, 852.
Habbal, S.R., *et al.*: 2001, *Obs. Travaux* **53**, 22.
Hansen, R.T., *et al.*: 1969, *Solar Phys.* **7**, 417.
Hewish, A.: 1972, In: Sonnett, C.P., Coleman, P.J. Jr., Wilcox, J.M. (eds.) *Solar Wind Three*, *NASA SP* **308**, NASA, Washington, 477.
Hundhausen, A.J.: 1977, In: Zirker, J.B. (ed.) *Coronal Holes and High Speed Streams*, Colorado Associated University Press, Boulder, 225.
Koutchmy, O., Koutchmy, S.: 1989, In: von der Lühe, O. (ed.) *10th SPO Workshop Proceedings*, NSO, 217.
Koutchmy, S., Bouchard, O., Mouette, J., Koutchmy, O.: 1993, *Solar Phys.* **148**, 169.
Koutchmy, S., *et al.*: 1992, *Astron. Astrophys. Suppl. Ser.* **96**, 169.
Koutchmy, S., *et al.*: 2001, *Obs. Travaux* **53**, 35.
Mentzel, D.H.: 1959, *Our Sun*, Harvard University Press, Cambridge, 189.
Morgan, H., Habbal, S.R., Woo, R.: 2006, *Solar Phys.* **236**, 263.
Munro, R., Jackson, B.V.: 1977, *Astrophys. J.* **213**, 874.
Newkirk, G. Jr.: 1967, *Rev. Astron. Astrophys.* **5**, 213.
Newkirk, G. Jr., Harvey, J.: 1968, *Solar Phys.* **3**, 321.
Newkirk, G. Jr., Dupree, R.G., Schmahl, E.J.: 1970, *Solar Phys.* **15**, 15.
November, L.J., Koutchmy, S.: 1996, *Astrophys. J.* **466**, 512.
Roelof, E.C., Pick, M.: 1989, *Astron. Astrophys.* **210**, 417.

Saito, K.: 1965, *Proc. Astron. Soc. Japan* **17**, 1.
Sheeley, N.R. Jr., *et al.*: 1997, *Astrophys. J.* **484**, 472.
Uchida, Y., *et al.*: 1992, *Publ. Astron. Soc. Japan* **44**, L155.
Van de Hulst, H.C.: 1950, *Bull. Astron. Inst. Netherlands* **11**, 150.
Woo, R.: 1978, *Astrophys. J.* **219**, 727.
Woo, R.: 1996a, *Astrophys. J.* **464**, L95.
Woo, R.: 1996b, *Nature* **379**, 321.
Woo, R.: 2005, *Solar Phys.* **231**, 71.
Woo, R.: 2006, *Astrophys. J.* **639**, L95.
Woo, R., Armstrong, J.W.: 1979, *J. Geophys. Res.* **84**, 7288.
Woo, R., Armstrong, J.W., Gazis, P.R.: 1995, *Space Sci. Rev.* **72**, 223.
Woo, R., Habbal, S.R.: 1997a, *Astrophys. J.* **474**, L139.
Woo, R., Habbal, S.R.: 1997b, *Geophys. Res. Lett.* **24**, 1159.
Woo, R., Habbal, S.R.: 2001, *Space Sci. Rev.* **97**, 81.
Woo, R., Habbal, S.R.: 2005, *Astrophys. J.* **629**, L129.
Woo, R., Habbal, S.R., Feldman, U.: 2004, *Astrophys. J.* **612**, 1171.
Wu, C.S., Reiner, M.J., Yoon, P.H., Zheng, H.N., Wang, S.: 2004, *Astrophys. J.* **605**, 503.